ASIAN JOURNAL OF CIVIL ENGINEERING (BUILDING AND HOUSING) VOL. 6, NO. 3 (2005)
PAGES 153-165

DERIVATION OF INCOMPATIBLE MODES IN NON-CONFORMING FINITE ELEMENTS USING HIERARCHICAL SHAPE FUNCTIONS

B. Hassani*[a] and S.M. Tavakkoli[b]
[a]School of Engineering, University of Wales Swansea, Room 155F, SA2 8PP, Swansea, UK
[b]Civil Engineering Department, Shahrood University of Technology, Shahrood 36155, Iran

ABSTRACT

The close relationship between the hierarchical shape functions and the incompatible modes in non-conforming finite elements is investigated and a simple approach is presented to systematically derive the incompatible modes of any order. The performance of the developed non-conforming elements is demonstrated via examples from literature and in comparison with the hybrid stress elements.

Keywords: finite elements, non-conforming, incompatible modes, hierarchical shape functions

1. INTRODUCTION

In order to increase the accuracy of a finite element analysis elements of higher order, either standard or hierarchical, are employed. However, this affects the computational cost of the analysis quite dramatically. The main idea in using the non-conforming finite elements is adding a few incompatible modes to the approximation polynomials of each element in order to overcome the problem of the over stiffness of the lower order elements. The coefficients of the incompatible modes are later condensed out from the formulation and consequently, the size of the resulting system of equations is kept unaffected.

Since the introduction of the incompatible modes in lower order finite element analysis by Wilson et al [1] in 1973, an enormous amount of research has been devoted to the development and improvement of the performance of the so called non-conforming finite elements. For example, see references [2-4,7]. Although the relationship between the incompatible displacement modes and the hierarchical shape functions has alluded by a few researchers, e.g. in [8], to the best knowledge of the authors, the derivation of these modes has been regarded as an intuitive and ad hoc one. This paper aims to present a simple approach to derive the incompatible modes from the hierarchical shape functions up to any

* E-mail address of the corresponding author: b_hassani@Computermail.net

order and in a systematic way.

2. INCOMPTIBLE DISPLACEMENT MODES

In the standard rfinite element formulation, the consistency between adjacent elements is provided via the satisfaction of the essential and natural boundary conditions for individual elements. In practice, this is achieved by using the global degrees of freedom together with the common process of assembling the global coefficient matrix [8]. However, in the non-conforming elements, due to the existence of a few extra parameters, the above condition between adjacent elements is not satisfied. Therefore, in the case of using the incompatible displacement modes, the consistency condition, in general, is violated. This means that a gap between adjacent elements can exist and therefore, the criteria of limited strains at the element edges are not guaranteed [7].

To clarify the problem, the following general single value partial differential equation for a boundary value problem is considered

$$\begin{aligned} &\boldsymbol{A}\,(u)=f\,, \\ &u=\bar{u} \qquad on \qquad \Gamma_u\,, \\ &c(\frac{\partial u}{\partial n})=t \qquad on \qquad \Gamma_t\,. \end{aligned} \tag{1}$$

Where $\boldsymbol{A}$ is a general differential operator, u is the primary variable, c is a coefficient, n is the normal unit vector, t is the secondary variable and Γ_u and Γ_t are the essential and natural boundaries of the problem. In the standard finite element method, the primary variable, u, is approximated as

$$u=\sum_{i=1}^{n} N_i u_i \tag{2}$$

Where N_i are the standard shape functions and n is the number of nodes per element. In the non-conforming elements the element displacements are expressed as the sum of compatible part u^c and the incompatible part u^n, which are approximated as below

$$u^c=\sum_{i=1}^{n} N_i^c u_i^c \tag{3}$$

$$u^n=\sum_{i=1}^{m} N_i^n a_i \tag{4}$$

One should note that in (3) N_i^c are the same as the n standard bilinear shape functions of an element, N_i^n in (4) are the m incompatible shape functions and a_i are the incompatible

modes' interpolation parameters.

As was mentioned above, adding the incompatible displacement modes violates the consistency condition. In other words, the displacement compatibility would not exist at the edges of elements any more. In addition, according to the convergence criteria, by decreasing the size of elements such that the size tends to zero, in the limit, a constant stress condition is realized. In this case, since the displacements are linear, the effects of the incompatible modes need to be eliminated. The above conditions for non-conforming elements are discussed in the following section.

2.1 Consistency condition

To alleviate the effects of inconsistency in the non-conforming elements and to increase the accuracy of solution, the discontinuity needs to be weakened as much as possible. The common approach for achieving this is to delete the effects of inconsistency from the formulation. For example, in the virtual displacement formulation the work done by the element edge traction forces due to the incompatible displacement modes disappears. A similar approach can be followed when the total potential energy functional is used [5].

Applying this idea to the boundary value problem (1) and discretizing the domain of interest into a mesh of finite elements, results in

$$\int_{\Gamma^e} N_i^n t d\Gamma = \int_{\Gamma^e} N_i^n c(\frac{\partial u^n}{\partial n}) d\Gamma = 0 \tag{5}$$

where Γ^e represents the total boundary of element e and n_x and n_y are the direction cosines of the boundary normal vectors. Since

$$\frac{\partial u^n}{\partial n} = n_x(\frac{\partial u^n}{\partial x}) + n_y(\frac{\partial u^n}{\partial y}) + n_z(\frac{\partial u^n}{\partial z})$$

and to ensure condition (5) it is sufficient to write

$$\int_{\Gamma^e} N_i^n n_x \frac{\partial u^n}{\partial x} d\Gamma = \int_{\Gamma^e} N_i^n n_y \frac{\partial u^n}{\partial y} d\Gamma = \int_{\Gamma^e} N_i^n n_z \frac{\partial u^n}{\partial z} d\Gamma = 0 \tag{6}$$

Equation (6) will be used later in order to obtain the appropriate incompatible modes from the hierarchical shape functions.

2.2. Convergence criteria

As the size of the finite elements become smaller and smaller, in the limit, a constant stress condition appears. The chosen approximate function should be such as to allow this to happen. In other words, one of the criteria for convergence is to satisfy the constant strain condition, which is equivalent to the passing of the constant stress patch tests. In the non-conforming elements with incompatible modes, the above criterion implies that in the case

of constant stresses, the strain energy induced by the incompatible modes should be zero [5,7]. By implementing the consistency condition as well as the convergence criteria, the well-known elements with incompatible modes [7] have been developed.

3. DERIVATION OF INCOMPATIBLE MODES

To improve the accuracy of the FE solution, the order of elements may be increased. Adding the appropriate hierarchical shape functions to the standard bilinear shape functions of the isoparametric plane stress elements can do this. By doing this, the approximated displacement function **u** can be written as

$$\mathbf{u} = \mathbf{u}^s + \mathbf{u}^h = \sum_{i=1}^{n} \mathbf{N}_i^s \mathbf{u}_i + \sum_{j=1}^{m} \mathbf{N}_j^h \mathbf{a}_j \tag{7}$$

where N_i^s and N_j^h are the standard and the hierarchical shape functions, respectively, and n and m are the number of them in the approximation.

When second order hierarchical shape functions are used, which is equivalent to the implementation of the eight node serendipity quadratic element, the incompatible modes suggested by Wilson [1, 2] are derived by following the procedure below. A systematic approach to the derivation of the incompatible modes in a more general sense is explained here. In this further development, in order to increase the accuracy, the quadratic and cubic hierarchical shape functions are employed. Therefore, by distinguishing the second and third order hierarchical shape function $\mathbf{u}^h$ in (7) can be written as $\mathbf{u}^h = \mathbf{u}^{h1} + \mathbf{u}^{h2}$.

In the case of a quadrilateral plane element $\mathbf{u}^{h1}$ and $\mathbf{u}^{h2}$ are

$$\mathbf{u}^{h1} = \sum_{i=1}^{4} \mathbf{N}_i^{h1} \bar{\mathbf{a}}_i \tag{8}$$

and

$$\mathbf{u}^{h2} = \sum_{i=1}^{4} \mathbf{N}_i^{h2} \bar{\mathbf{b}}_i \tag{9}$$

where, $\mathbf{N}_i^{h1}$, $\bar{\mathbf{a}}_i$, $\mathbf{N}_i^{h2}$ and $\bar{\mathbf{b}}_i$ are the hierarchical shape functions and interpolation parameters for second and third order approximations, respectively. By using the second order hierarchical shape functions, (8) can be written as

$$\begin{aligned} \mathbf{u}^{h1} = {} & \frac{1}{2}(1-\xi^2)(1+\eta)\bar{\mathbf{a}}_1 + \frac{1}{2}(1-\xi)(1-\eta^2)\bar{\mathbf{a}}_2 + \\ & \frac{1}{2}(1-\xi^2)(1-\eta)\bar{\mathbf{a}}_3 + \frac{1}{2}(1+\xi)(1-\eta^2)\bar{\mathbf{a}}_4 \end{aligned} \tag{10}$$

It is noted that parameters $\bar{\mathbf{a}}_i$ represent the magnitude of the departure from a linear approximation at the center of the edges of a quadrilateral element.

Similarly, $\mathbf{u}^{h2}$ can be written as

$$\mathbf{u}^{h2} = \frac{1}{2}\xi\eta(1-\xi^2)(1+\eta)\bar{\mathbf{b}}_1 + \frac{1}{2}\xi\eta(\xi-1)(1-\eta^2)\bar{\mathbf{b}}_2 + \frac{1}{2}\xi\eta(1-\xi^2)(\eta-1)\bar{\mathbf{b}}_3 + \frac{1}{2}\xi\eta(1+\xi)(1-\eta^2)\bar{\mathbf{b}}_4 \ . \tag{11}$$

The shape functions in (11) are chosen in such a way that they are zero at the middle and corners of the edges of a typical bilinear quadrilateral element. Also, the slope at the middle of each edge is unity. One should note that, in general, these shape functions are not unique and different ones might be used.

Now, by substituting the hierarchical displacements $\mathbf{u}^{h1}$ and $\mathbf{u}^{h2}$ and the related shape functions from (10) and (11) in place of $\mathbf{u}^{n}$ and $\mathbf{N}_i^{n}$ in (6) we can write

$$\int_{\Gamma_e} \mathbf{N}_i^{n1} n_x \frac{\partial \mathbf{u}^{n1}}{\partial x} d\Gamma = \int_{\Gamma_e} \mathbf{N}_i^{n1} n_y \frac{\partial \mathbf{u}^{n1}}{\partial y} d\Gamma = 0 \tag{12}$$

$$\int_{\Gamma_e} \mathbf{N}_i^{n2} n_x \frac{\partial \mathbf{u}^{n2}}{\partial x} d\Gamma = \int_{\Gamma_e} \mathbf{N}_i^{n2} n_y \frac{\partial \mathbf{u}^{n2}}{\partial y} d\Gamma = 0 \tag{13}$$

which are the implementation of the idea at two stages for the hierarchical shape functions of different orders. According to the above equations and by substituting equations (10) and (11) in (12) and (13), it is noted that the interpolation parameters of the hierarchical shape functions are related to each other and are not independent. To simplify the problem, the above equations are solved for the case of elements with a constant Jacobian, e.g. rectangular elements. In doing so, the following relations are easily resulted

$$\bar{\mathbf{a}}_1 = \bar{\mathbf{a}}_3 = \mathbf{a}_1 \quad , \quad \bar{\mathbf{a}}_2 = \bar{\mathbf{a}}_4 = \mathbf{a}_2 \tag{14}$$

and

$$\bar{\mathbf{b}}_1 = \bar{\mathbf{b}}_3 = \mathbf{b}_1 \quad , \quad \bar{\mathbf{b}}_2 = \bar{\mathbf{b}}_4 = \mathbf{b}_2 \ . \tag{15}$$

Now, by using (14) and (15), equations (10) and (11) can be written as

$$\mathbf{u}^{n1} = (1-\xi^2)\mathbf{a}_1 + (1-\eta^2)\mathbf{a}_2 \ , \tag{16}$$

$$\mathbf{u}^{n2} = \xi\eta^2(1-\xi^2)\mathbf{b}_1 + \xi^2\eta(1-\eta^2)\mathbf{b}_2 \, . \tag{17}$$

In the equations above, the coefficients of the parameters $\mathbf{a}_1, \mathbf{a}_2, \mathbf{b}_1$ and $\mathbf{b}_2$ are often

referred to as *incompatible shape functions*.

Following a similar procedure, in the case of three-dimensional eight node brick element and choosing the second and third order hierarchical shape functions as

$$\begin{aligned}
N_1^{h1} &= (1/4)(1-\xi)(1-\eta^2)(1+\zeta), & N_2^{h1} &= (1/4)(1-\xi^2)(1-\eta)(1+\zeta) \ , \\
N_3^{h1} &= (1/4)(1+\xi)(1-\eta^2)(1+\zeta), & N_4^{h1} &= (1/4)(1-\xi^2)(1+\eta)(1+\zeta) \ , \\
N_5^{h1} &= (1/4)(1-\xi)(1+\eta)(1-\zeta^2), & N_6^{h1} &= (1/4)(1-\xi)(1-\eta)(1-\zeta^2) \ , \\
N_7^{h1} &= (1/4)(1+\xi)(1-\eta)(1-\zeta^2), & N_8^{h1} &= (1/4)(1+\xi)(1+\eta)(1-\zeta^2) \ , \\
N_9^{h1} &= (1/4)(1-\xi)(1-\eta^2)(1-\zeta), & N_{10}^{h1} &= (1/4)(1-\xi^2)(1-\eta)(1-\zeta) \ , \\
N_{11}^{h1} &= (1/4)(1+\xi)(1-\eta^2)(1-\zeta), & N_{12}^{h1} &= (1/4)(1-\xi^2)(1+\eta)(1-\zeta) \ .
\end{aligned} \tag{18}$$

and

$$\begin{aligned}
N_1^{h2} &= (1/4)(\xi\eta\zeta)(-1+\xi)(1-\eta^2)(1+\zeta), & N_2^{h2} &= (1/4)(\xi\eta\zeta)(1-\xi^2)(-1+\eta)(1+\zeta), \\
N_3^{h2} &= (1/4)(\xi\eta\zeta)(1+\xi)(1-\eta^2)(1+\zeta), & N_4^{h2} &= (1/4)(\xi\eta\zeta)(1-\xi^2)(1+\eta)(1+\zeta), \\
N_5^{h2} &= (1/4)(\xi\eta\zeta)(-1+\xi)(1+\eta)(1-\zeta^2), & N_6^{h2} &= (1/4)(\xi\eta\zeta)(1-\xi)(1-\eta)(1-\zeta^2), \\
N_7^{h2} &= (1/4)(\xi\eta\zeta)(1+\xi)(-1+\eta)(1-\zeta^2), & N_8^{h2} &= (1/4)(\xi\eta\zeta)(1+\xi)(1+\eta)(1-\zeta^2), \\
N_9^{h2} &= (1/4)(\xi\eta\zeta)(1-\xi)(1-\eta^2)(1-\zeta), & N_{10}^{h2} &= (1/4)(\xi\eta\zeta)(1-\xi^2)(1-\eta)(1-\zeta), \\
N_{11}^{h2} &= (1/4)(\xi\eta\zeta)(1+\xi)(1-\eta^2)(-1+\zeta), & N_{12}^{h2} &= (1/4)(\xi\eta\zeta)(1-\xi^2)(1+\eta)(-1+\zeta).
\end{aligned} \tag{19}$$

results in

$$\mathbf{u}^{n1} = \sum_{i=1}^{m=3} \mathbf{N}_i^{n1}\mathbf{a}_i = (1-\xi^2)\mathbf{a}_1 + (1-\eta^2)\mathbf{a}_2 + (1-\zeta^2)\mathbf{a}_3 \tag{20}$$

$$\mathbf{u}^{n2} = \sum_{i=1}^{n=3} \mathbf{N}_i^{n2}\mathbf{b}_i = \xi\eta^2\zeta^2(1-\xi^2)\mathbf{b}_1 + \xi^2\eta\zeta^2(1-\eta^2)\mathbf{b}_2 + \xi^2\eta^2\zeta(1-\zeta^2)\mathbf{b}_3 \tag{21}$$

Considering (16) and (20), it is observed that the shape functions are exactly the incompatible modes suggested by Wilson and Taylor [1, 2]. Also, noted that $\mathbf{N}^{\mathrm{hi}}$ are renamed as $\mathbf{N}^{\mathrm{n}}$ from now on.

4. FINITE ELEMENT FORMULATION

The approximated displacement functions $\mathbf{u} = \left\langle \mathrm{u_x}, \mathrm{u_y} \right\rangle^{\mathrm{T}}$ for a four-node isoparametric element with four incompatible modes for each component of displacement can be written as

$$\mathbf{u} = \sum_{i=1}^{4} \mathbf{N}_i \bar{\mathbf{u}}_i + \sum_{i=1}^{2} \mathbf{N}_i^{n1} \mathbf{a}_i + \sum_{i=1}^{2} \mathbf{N}_i^{n2} \mathbf{b}_i \tag{22}$$

or

$$\mathbf{u} = \mathbf{N}\bar{\mathbf{u}} + \mathbf{N}^{n1}\mathbf{a} + \mathbf{N}^{n2}\mathbf{b} \ . \tag{23}$$

Using (23) the element strains can be written as

$$\boldsymbol{\varepsilon} = \mathbf{B}\bar{\mathbf{u}} + \mathbf{B}_1\mathbf{a} + \mathbf{B}_2\mathbf{b} \ , \tag{24}$$

where $\mathbf{B}$, $\mathbf{B}_1$ and $\mathbf{B}_2$ are the strain-displacement matrices. Also the stress-strain relationship is

$$\boldsymbol{\sigma} = \mathbf{D}\boldsymbol{\varepsilon} \tag{25}$$

where $\mathbf{D}$ is the elasticity matrix.

Following a standard approach for the derivation of the finite elements formulation, the matrix of coefficients can easily be obtained. For example, by implementing the virtual displacement method for a typical element with body forces $\mathbf{b}$ and traction forces $\mathbf{t}$ we have

$$\int_{\Omega^e} \delta\boldsymbol{\varepsilon}^T \boldsymbol{\sigma} \ d\Omega - \int_{\Omega^e} \delta\mathbf{u}^T \mathbf{b} \ d\Omega - \int_{\Gamma^e} \delta\mathbf{u}^T \mathbf{t} \ d\Gamma = 0 \ , \tag{26}$$

and using (24) the variation of $\boldsymbol{\varepsilon}$ is obtained as

$$\delta\boldsymbol{\varepsilon} = \mathbf{B}\delta\bar{\mathbf{u}} + \mathbf{B}_1\delta\mathbf{a} + \mathbf{B}_2\delta\mathbf{b} \tag{27}$$

Now, substituting from (21), (22) and (27) into the first term of (26) and using $\delta\mathbf{u} = \mathbf{N}\delta\bar{\mathbf{u}}$ for the other terms, and ignoring the coefficient of $\delta\bar{\mathbf{u}}^{\mathrm{T}}, \delta\mathbf{a}^{\mathrm{T}}$ and $\delta\mathbf{b}^{\mathrm{T}}$ results in a system of three equations which in matrix form can be shown as

$$\begin{bmatrix} \mathbf{K} & \mathbf{E}_1^T & \mathbf{E}_2^T \\ \mathbf{E}_1 & \mathbf{H}_1 & \mathbf{E}_3^T \\ \mathbf{E}_2 & \mathbf{E}_3 & \mathbf{H}_2 \end{bmatrix} \begin{bmatrix} \bar{\mathbf{u}} \\ \mathbf{a} \\ \mathbf{b} \end{bmatrix} = \begin{bmatrix} \mathbf{f} \\ \mathbf{0} \\ \mathbf{0} \end{bmatrix} \tag{28}$$

where

$$\begin{aligned} \mathbf{K} &= \int_{V^e} \mathbf{B}^T\mathbf{D}\mathbf{B} \ dV \ , & \mathbf{E}_3 &= \int_{V^e} \mathbf{B}_2^T\mathbf{D}\mathbf{B}_1 \ dV \ , \\ \mathbf{E}_1 &= \int_{V^e} \mathbf{B}_1^T\mathbf{D}\mathbf{B} \ dV \ , & \mathbf{H}_1 &= \int_{V^e} \mathbf{B}_1^T\mathbf{D}\mathbf{B}_1 \ dV \ , \\ \mathbf{E}_2 &= \int_{V^e} \mathbf{B}_2^T\mathbf{D}\mathbf{B} \ dV \ , & \mathbf{H}_2 &= \int_{V^e} \mathbf{B}_2\mathbf{D}\mathbf{B}_2 \ dV \ , \end{aligned} \tag{29}$$

and

$$\mathbf{f} = \int_{\Omega^e} \mathbf{N}^T \mathbf{b} \quad d\Omega + \int_{\Gamma^e} \mathbf{N}^T \mathbf{t} \quad d\Gamma \quad . \tag{30}$$

As mentioned in Section 2.2, the convergence criteria need to be satisfied which is equivalent to passing the constant stress patch test [7]. Since equations (28) may not satisfy the convergence criteria, some corrections on the terms as defined in (29) are in order. This can be achieved by neglecting the contribution of the incompatible modes in the internal virtual work as shown in equations (26). Thus

$$\delta \mathbf{a}^T \left(\int_{\Omega^e} \mathbf{B}_1^T \boldsymbol{\sigma} \quad d\Omega \right) = 0 \quad , \tag{31}$$

$$\delta \mathbf{b}^T \left(\int_{\Omega^e} \mathbf{B}_2^T \boldsymbol{\sigma} \quad d\Omega \right) = 0 \quad . \tag{32}$$

Considering $\boldsymbol{\sigma}$ to be constant, from (31) and (32) it can be concluded that we should have

$$\int_{\Omega^e} \mathbf{B}_1^T \quad d\Omega = 0 \quad , \tag{33}$$

$$\int_{\Omega^e} \mathbf{B}_2^T \quad d\Omega = 0 \quad . \tag{34}$$

Considering the definition of the $\mathbf{B}$ matrix, it can easily be shown that (33) and (34) can also be written as

$$\int_{\Omega^e} \mathbf{B}_1 \quad d\Omega = 0 \qquad \text{and} \qquad \int_{\Omega^e} \mathbf{B}_2 \quad d\Omega = 0 \quad . \tag{35}$$

Equations (35) can be satisfied by adding constant correction matrices $\mathbf{B}_1^c$ and $\mathbf{B}_2^c$ to them. Therefore,

$$\int_{\Omega^e} (\mathbf{B}_1 + \mathbf{B}_1^c) \quad d\Omega = \int_{\Omega^e} \overline{\mathbf{B}}_1 \quad d\Omega = 0 \quad , \tag{36}$$

$$\int_{\Omega^e} (\mathbf{B}_2 + \mathbf{B}_2^c) \quad d\Omega = \int_{\Omega^e} \overline{\mathbf{B}}_2 \quad d\Omega = 0 \quad , \tag{37}$$

where

$$\overline{\mathbf{B}}_1 = \mathbf{B}_1 + \mathbf{B}_1^c \, , \qquad \overline{\mathbf{B}}_2 = \mathbf{B}_2 + \mathbf{B}_2^c \, . \tag{38}$$

From (36) and (37) the constant correction matrices can easily be calculated as

$$\mathbf{B}_1^c = \frac{-1}{\Omega^e} \int_{\Omega^e} \mathbf{B}_1 \quad d\Omega \quad , \tag{39}$$

$$\mathbf{B}_2^c = \frac{-1}{\Omega^e}\int_{\Omega^e} \mathbf{B}_2 \quad d\Omega \quad . \tag{40}$$

Therefore, in order to be able to reach the constant stress state, in (28) and (29), $\overline{\mathbf{B}}_1$ and $\overline{\mathbf{B}}_2$ should be used in place of $\mathbf{B}_1$ and $\mathbf{B}_2$

Additionally, for the constant stress case, $\boldsymbol{\sigma}$, in its general form, can be written as

$$\boldsymbol{\sigma} = \mathbf{DB}\overline{\mathbf{u}} + \mathbf{DB}_1\mathbf{a} \; . \tag{41}$$

It should be noted that by considering a higher order extra term in (41), it is impossible to reach a constant stress state. From this point, it follows that in (24) and (25) the matrix $\mathbf{H}_2$ does not need any correction. Thus, (28) will be changed to

$$\begin{bmatrix} \mathbf{K} & \overline{\mathbf{E}}_1^{\,T} & \overline{\mathbf{E}}_2^{\,T} \\ \overline{\mathbf{E}}_1 & \overline{\mathbf{H}}_1 & \overline{\mathbf{E}}_3^{\,T} \\ \overline{\mathbf{E}}_2 & \overline{\mathbf{E}}_3 & \mathbf{H}_2 \end{bmatrix} \begin{bmatrix} \overline{\mathbf{u}} \\ \mathbf{a} \\ \mathbf{b} \end{bmatrix} = \begin{bmatrix} \mathbf{f} \\ \mathbf{0} \\ \mathbf{0} \end{bmatrix} \quad , \tag{42}$$

Where the bar superscript denotes the corrected matrices. From (42) it is observed that the incompatible mode parameters $\mathbf{a}$ and $\mathbf{b}$ can be omitted by a conventional static condensation procedure. This results in the equivalent stiffness matrix $\overline{\mathbf{K}}$ where

$$\overline{\mathbf{K}} = \mathbf{K} - \begin{bmatrix} \overline{\mathbf{E}}_1 & \overline{\mathbf{E}}_2 \end{bmatrix}^T \begin{bmatrix} \overline{\mathbf{H}}_1 & \overline{\mathbf{E}}_3 \\ \overline{\mathbf{E}}_3 & \mathbf{H}_2 \end{bmatrix}^{-1} \begin{bmatrix} \overline{\mathbf{E}}_1 & \overline{\mathbf{E}}_2 \end{bmatrix} \; . \tag{43}$$

5. NUMERICAL EXAMPLES

Three examples are presented to demonstrate the accuracy of the developed non-conforming element. The results are compared with different methods, which are employed in our developed finite element code.

Example 1: The cantilever beam of Figure 1, which was solved in [5, 6,7], is considered under two load cases: 1) an end moment at the free edge of the beam and 2) a vertical shear load at the free edge. The beam is discretized by five trapezoidal elements as illustrated in Figures 1.a and 1.b.

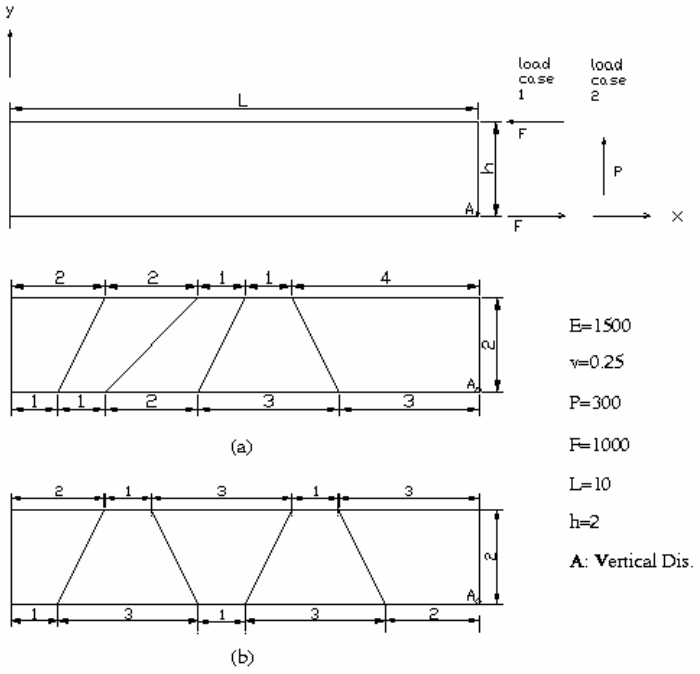

Figure 1. Cantilever beam (a) Distorted mesh (b) Trapeziodal mesh

In Table 1, the resulting vertical displacements for the bottom corner of the free edge of the cantilever beam (point A in Figure 1) are compared with those obtained from implementing different methods. The reported values and their references are also provided in parentheses.

Table 1. Cantilever beam Figure 1

Mesh			Distorted	Trapeziodal
	Element	Load Case	Vertical Displacement	Vertical Displacement
	Compatible	1	45.65	54.77
	Wilson's	1	96.00 (95.8 [5])	76.25
	Hybrid 5B-A	1	96.10 (96.49 [6])	70.04
	Present	1	98.39	79.59
	Exact	1	100	100
	Compatible	2	50.96	59.05
	Wilson's	2	97.95 (97.7 [5])	80.12
	Hybrid 5B-A	2	98.14 (98.37 [6])	73.65
	Present	2	100.49	82.90
	Exact	2	102.6	102.6

Example 2: A plane stress curved cantilever beam under end shear load, as depicted in Figure 2, is considered. Four trapezoidal elements are used for discretizing the domain of the problem. The modulus of elasticity and Poisson's ratio are assumed to be 1000 and 0.3, respectively. The obtained results are shown in Table 2.

Table 2. Circular beam Figure 2

Element	Horizental Displacement
Compatible	59.93
Wilson's	86.77
Hybrid 5B -A	88.51
Present (MIE)	87.45
Exact	90.41

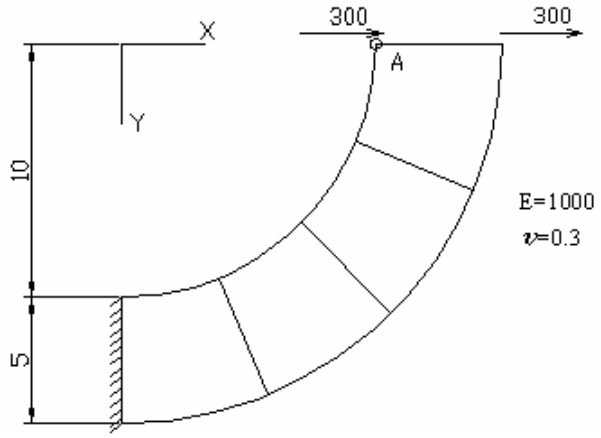

Figure 2. Circular beam under end shear load

Example 3: A twisted beam under end shear load, as illustrated in Figure 3, is considered. 36 brick elements are used for discretizing of the domain of problem. The modulus of elasticity E and the Poisson's ratio are assumed to be 29.0E6 and 0.22, respectively. Length, width and depth of the beam are 12.0, 1.1 and 0.32 respectively and the angle of twist is 90 degrees. The obtained results are shown in Table 3.

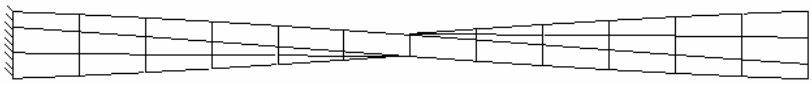

Figure 3. Twisted 3D beam

Table 3. Twisted 3D Beam

Element	Out-of-plane shear	In-plane shear
Compatible	0.000582694	0.00111884
Wilson's	0.001730193	0.005384828
Hybrid	0.001755258	0.00545427
Present	0.001734881	0.005405259
Exact	0.001754	0.005424

6. CONCLUSION

The so-called incompatible displacement modes are closely related to the hierarchical shape functions. As demonstrated in this paper, they can be obtained in a systematic approach and up to any desired order. By adding extra incompatible modes to the approximation polynomials, more accurate results are obtained. As it is expected, the relative improvement in the accuracy of the results, by using higher order modes in comparison with the quadratic incompatible mode shapes, is reduced.

REFERENCES

1. Wilson, E.L. and Taylor, R.L. and Doherty, W. P. and Gabouss, J., Incompatible displacement models, In Fenves, S.J. et al, eds, *Numerical and Computer Methods in Structural Mechanics,* Academic Press, New York, 1973, pp. 43-57.
2. Taylor, R.L. and Wilson, E.L., A non conforming element for stress analysis, *International Journal for Numerical Methods in Engineerin*g, **10**(1976)1211-1219.
3. Simo, J.C. and Rifai, M.S., A class of mixed assumed strain methods and the method of incompatible modes, *International Journal for Numerical Methods in Engineerin*g, **29**(1990)1595-1638.
4. Wanji, C. and Cheung, Y.K., A robust refined quadrilateral plane element', *International Journal for Numerical Methods in Engineerin*g, **38**(1995)649-666.
5. Wilson, E.L. and Ibrahimbegovic, A., Use of incompatible displacement modes for the calculation of element stiffnesses or stresses, *Finite Elements in Analysis and Design*, **7**(1990)229-241.
6. Yuan, K.Y. and Huang Y.S. and Pian T. H. H., New strategy for assumed stresses for 4-node hybrid stress Membrane Element, *International Journal for Numerical Methods in Engineerin*g, **36**(1993)1747-1763.
7. Wu, C.C. and Huang, M.G. and Pian T. H. H., Consistency Condition and Convergence

Criteria of Incompatible Elements: General Formulation of Incompatible Functions and its Application, *Computers and Structures*, **27**(1987)639-644.

8. Zienkiewicz, O.C. and Taylor, R.L., *The Finite Element Method*, Vol. 1, 5th edn, McGraw-Hill, London, 2000.